

Ion-assist applications of broad-beam ion sources

H.R. Kaufman^a and J.M.E. Harper^b

^aKaufman & Robinson, Inc., 1306 Blue Spruce Dr., Fort Collins, CO 80524;

^bUniversity of New Hampshire, Dept. of Physics, DeMeritt Hall 207, Durham, NH 03824

ABSTRACT

Ion-assist applications of broad-beam ion sources are reviewed for ion energies up to about 1 keV. These applications are organized by ion energy and cover a wide range of thin-film technologies. Optimum ion-assist doses are described when available. Except for applications that benefit from specific ion energies, the majority of ion-assist applications are probably done best in the low-energy range that extends from about 25 eV to 100 eV.

Keywords: Ion sources, ion assist, deposition, IAD, thin films.

1. INTRODUCTION

Ion-assist applications in thin films are closely tied to the use of industrial ion sources. Almost all of the fundamental studies of ion-assist processes and most of the subsequent applications have used these sources. Industrial applications of broad-beam ion sources became significant starting about 1970.¹ The early ion sources were almost all gridded (utilizing electrostatic acceleration) and the applications involved mostly etching and deposition.² By 1982 many ion-beam assisted processes had been investigated including, for example, forming oxides and nitrides with oxygen and nitrogen ions, passivating polycrystalline silicon with hydrogen ions, increasing thin-film hardness and adhesion, incorporating inert working gas during deposition, and controlling thin-film stress.¹ With the increasing study of ion-assist applications, the benefits of low ion energies (approximately ≤ 100 eV) became apparent.

A variety of options were used to increase the current capability of gridded ion sources at low ion energies, including decreased grid spacing, increased numbers of apertures in each grid, three-grid ion optics, and one-grid optics.³ While one-grid optics did not have the durability to be used in other than very specialized production applications, they have been quite useful in research studies that helped quantify the importance of low ion energies.⁴⁻⁶ Another response to the need for higher ion currents at low ion energies was the development of gridless ion sources suitable for production environments.^{7,8} The continued and expanding interest in ion assisted applications has been reflected in the expanding scope of reviews of these applications.⁹⁻¹²

1.1 Ion-assist parameters

In addition to the element or compound that is deposited and the gas used to generate ions, the minimum information required to reproduce an ion-assist application is typically: the deposition rate (in $\text{\AA}/\text{s}$), the ion energy (in eV), and the ion current density (in mA/cm^2 or $\mu\text{A}/\text{cm}^2$). To facilitate comparison between different materials and processes, the ion current density is replaced herein with ion/atom ratio and the energy dose in eV/atom, where the atoms are the atoms that are deposited (including, for example, oxygen atoms when an oxide is being deposited). Some processes require additional parameters to characterize, but these additional parameters should supplement, not replace, the basic parameters of deposition rate, ion energy, ion/atom ratio, and ion energy per atom. From a rigorous information viewpoint, any two of ion energy, ion/atom ratio, and ion energy per atom will convey the same information. But the most convenient pair of these three depends on the application, and all three are often included for the reader's convenience. The ion-assist process papers reviewed herein were mostly limited to those that included these basic parameters, or at least sufficient information for their determination. Unless otherwise specified, the assist ions are Ar^+ and the films are vapor deposited. Unless the angle of incidence for the ions on the substrate is given, it is typically 20-30 degrees from normal. For compounds, the deposition rate given is always for the compound, even if that rate had to be calculated from the deposition rate of one element and the properties of that element and the resulting compound.

1.2 Organization by ion energy

To more accurately present and understand the applications reviewed herein, they have been organized by ion-assist energy. The upper limit of *very-low-energy applications* (~0-25 eV) corresponds roughly to the energy to displace atoms in the bulk lattice,^{10,13} as well as the approximate sputtering threshold for a variety of materials.¹⁴ Surface atoms, which are less tightly bound, can still be moved, and the movement of these surface atoms is the usual objective of an ion-assisted process in this energy regime. Ions in the very-low-energy range are usually supplied by plasma discharges of some kind,^{15,16} although end-Hall ion sources can operate at mean energies in this range with an upper limit for the distribution as low as 30 eV for Ar⁺ ions and 20 eV for Xe⁺ ions.¹⁷

Low-energy applications (~25-100 eV) include the fabrication of most high-density, low-implantation films. Studies have shown that near-bulk densities can be obtained with little gas implantation at ion energies less than about 100 eV and greater than about 25 eV.^{6,18-20} Metal films, where grain boundaries are easily moved, tend to show large crystallite sizes in the low-energy regime.¹⁸ The multiple-particle interactions of the molecular-dynamics approach most accurately represent the ion-assist processes in this regime,¹⁹ as opposed to the collision-cascade approach that is essentially a sequence of two-body collisions and is more applicable at energies greater than 1 keV. Consistent with the multiple-particle and lattice-vibration interactions of the molecular-dynamics approach, eV/atom appears to be the best measure of an ion-assist process in this regime.^{6,21} Many commercial ion-assisted films are fabricated in this energy range, where the end-Hall ion source^{7,8} is preferred because of the higher ion flux at low ion energy.

High-energy applications (~100-1000 eV) typically generate small crystallites and many lattice defects.^{10,13,18} High densities can be obtained, approaching those of the low-energy regime, but are obtained at the cost of many more defects. The desired properties in this regime can be high microhardness, high resistivity, or high gas incorporation, all of which increase continuously with ion energy. This is a transition region for processes, extending from the multiple-particle interactions of the molecular-dynamics approach at the lower limit to the two-body collision-cascade approach at the upper limit. Consistent with being a transition region, there is no single parametric approach (such as energy dose in eV/ion) that effectively correlates experimental results from different applications. This lack of correlation is shown clearly in the effect of ion assist on film stress (compare Sections 4.2.1 and 4.2.2). The lower limit of this energy range is somewhat arbitrary, with a gradual transition from the low-energy regime. The upper limit for ion energy (1000 eV) is more arbitrary. As a practical matter, however, many industrial broad-beam ion sources can generate energies of 1000 eV, but very few can generate energies >2000 eV. For those interested, there are reviews that include processes at higher ion energies.^{10,22} Early applications were often carried out at high energy because low-energy sources were not readily available. As low-energy ion sources became more available, fewer commercial ion-assisted films have been fabricated in the high-energy range. High-energy applications are distinguished from the energy-specific applications that follow by generally increasing in rate and/or intensity as ion energy increases from about 100 eV to about 1000 eV. At the low end of the energy range up to about 200 eV, the end-Hall ion source^{7,8} is preferred for generating ions. At higher energies, gridded ion sources are preferred.

The last category is *energy-specific applications*. These applications typically involve a selection, such as the selection of a particular molecular bond, or the selection of a particular molecular alignment. For effective selection to take place, the ion-assist energy must be near an optimum value, large enough to break some molecular bonds, or large enough to realign some crystallites, but small enough to avoid randomization of the structure. The optimum ion energy varies with the particular application, but, for the applications described, extends from less than 50 eV to over 1000 eV. Very-low-energy applications are not included because one of the objectives for those applications is avoiding lattice damage.

1.3 Gridded and gridless ion sources

The ion-beam current capabilities of typical gridded and gridless ion sources are indicated in Fig. 1(a), while the ion-beam power capabilities are indicated in Fig. 1(b). The working gas is Ar and the ions produced are mostly all Ar⁺, but the characteristics shown would not be greatly different for O₂ or N₂, where the ions would be mostly O₂⁺ and N₂⁺. The ion energies are mean values, although the difference between mean and maximum values is probably not significant except for ion energies below about 50 eV. Particular medium-sized gridded and gridless ion sources were used for these ion-

beam characteristics,^{23,24} but the same qualitative results could have been shown using the characteristics of other specific gridded and gridless ion sources. The upper limit for gridless ion energy is about 200 eV or less, and depends on the background pressure. Below this upper limit, the ion current of the gridless ion source is limited by discharge power, except at the lowest ion energies where it is limited by the ionization process. Note the rapid variation of ion-beam current, and even more rapid variation of ion-beam power, with ion energy for a gridded ion source. This rapid variation is due to the space-charge limit (Child's law²⁵) on electrostatic acceleration. For reasonable process rates with a gridded ion source, the compromise is often between inadequate current and power at low ion energies and excessive damage at high energies, with the optimum ion energy the lowest one at which the process rate is acceptable. Because the early ion sources were mostly gridded, many early ion assisted applications were carried out at high ion energies, when they could have been performed better at low ion energies. The ready availability of gridless ion sources has drastically altered the choices, permitting both high current and power at low ion energies, where there is little damage.

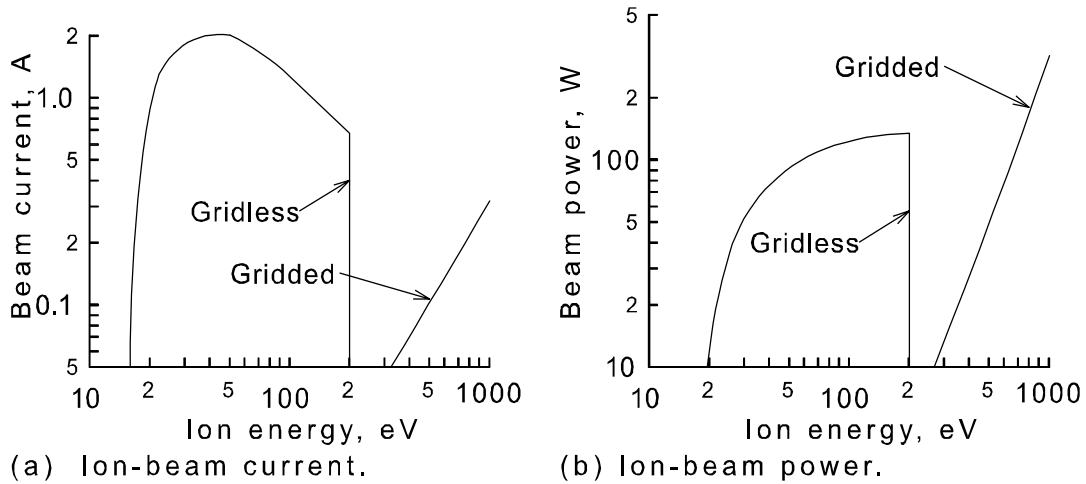


Fig. 1. Ion-beam characteristics for gridded²³ and gridless²⁴ ion sources.

2. VERY-LOW-ENERGY APPLICATIONS (~0-25 eV)

2.1 Cleaning semiconductors

The objectives in cleaning are to reduce contamination in, and improve adhesion to, subsequently deposited films. Semiconductors are particularly sensitive to damage and are therefore assumed to be in the very-low-energy category. The only example here is the cleaning of gallium arsenide, where the ion energy used was slightly higher than the upper limit for the very-low-energy category and surface damage was observed. Surfaces of GaAs were cleaned with Ar^+ ions.²⁶ These surfaces were evaluated by forming diodes on them. Small adverse changes in diode properties were observed when diodes were formed on surfaces after cleaning with 50 eV Ar^+ ions, compared to the properties of diodes formed on uncleaned surfaces. After cleaning, the original semiconductor properties were restored with a chemical etch of 17 Å, indicating damage to that depth. The small change in diode properties and the shallow depth of the damage both indicate that a short anneal might be effective in removing most of the damage. Also note that the objective here was to retain the original semiconductor properties. If the objective had been to make an ohmic contact with the semiconductor, cleaning with more energetic ions could have had beneficial side effects - see Section 5.4.

2.2 Very thin layers, sharp interfaces

Very thin deposited layers, such as used in giant magnetoresistive (GMR) materials or x-ray optics present special ion-assist problems. The general area of interest for ion energy is <20 eV.²⁷ Interface roughness and mixing can constitute a larger fraction of the total thickness of a thin layer, and thus have greater adverse effects than in thicker layers. The most thorough studies of the ion-assist control of roughness and mixing include comparisons with experiments, but are primarily theoretical - i.e., molecular dynamics simulations.²⁷⁻²⁹ This use of theoretical calculations is in contrast to most of the work cited in other sections herein, which is almost all experimental. The assumed final configuration had two 60 Å layers of Ni

separated by a 20 Å layer of Cu. The most critical fabrication steps would be the transitions from one material to the other, where the initial deposition of the new material would tend to form clumps or Islands before a continuous film would form. The effect of ion bombardment on the flattening of these islands and the mixing of island material with the underlying material was studied. Ion incidence was normal to the mean surface. The flattening and mixing thresholds are all below the "sputter threshold," the energy at which the sputter yield becomes very small, typically 20-30 eV for common elements.¹⁴

2.2.1 Cu on Ni. The cohesive energy of Cu is lower than Ni, which resulted in the flattening threshold for Cu islands on Ni (2 eV Ar⁺ and 1 eV for Xe⁺) being lower than the mixing threshold (15 eV Ar⁺ and 10 eV Xe⁺). Thus a range of 2-15 eV for Ar⁺ and 1-10 eV for Xe⁺ is available for flattening of initial Cu islands without significant mixing with the supporting surface of Ni. The flattening threshold for Ni on Ni (which simulated the flattening of the Ni layer before starting the Cu deposition) was 8 eV Ar⁺ and 6 eV Xe⁺. Saturation flattening was in all cases obtained at an ion/atom ratio of about 5.

2.2.2 Ni on Cu. The reverse situation occurred for Ni on Cu. The flattening threshold for Ni islands on Cu (14 eV Ar⁺ and 12 eV for Xe⁺) was higher than the mixing threshold (9 eV Ar⁺ and 5 eV Xe⁺). Thus no range existed where substantial flattening of Ni islands could be obtained without also having substantial and undesirable mixing with the supporting surface of Cu. The flattening threshold for Cu on Cu (which simulated the flattening of the Cu layer before starting the Ni deposition) was 4 eV Ar⁺ and 3 eV Xe⁺. Saturation flattening was again obtained at an ion/atom ratio of about 5. A "modulated" ion assist of Ni on Cu was proposed for obtaining flattening with reduced mixing. The first few monolayers of Ni should be deposited without ion assist. Then the ion assist should be started and continued for the rest of that layer. Another approach suggested to reduce mixing was to deposit a buffer layer on the Cu before depositing the Ni. For Cu, Co was suggested because it is "thermodynamically immiscible" with Cu.

2.2.3 Other materials and processes. From the above theoretical studies of Cu and Ni,²⁷⁻²⁹ a transition from a material with a greater cohesive energy to one with a lesser cohesive energy should be relatively easy. Conversely, care should be used whenever there is a transition from a material with a lesser cohesive energy to one with a greater cohesive energy. Some cohesive energies given in eV were, in order of increasing energy: Ag, 2.85; Cu, 3.54; Au, 3.93; and Ni, 4.45. A relative order of cohesive energies (ΔH^a) for additional materials, with slightly different numerical values, is available from another source.³⁰ Although the work described in this section²⁷⁻²⁹ is directly applicable to the very-low-energy regime, it also has important implications for low-energy processes where better interface definition is needed. As examples, one layer can be well flattened before starting the next layer, surface temperature can be minimized to produce a large number of small islands (rather than fewer large islands) at the start of the next layer, and modulated ion assist can be used, waiting until the equivalent of several monolayers of the next layer is deposited before restarting ion assist.

2.3 Control of microstructure

2.3.1 α -phase tantalum - sputter deposited Ta. Films of Ta were deposited to a thickness of 300 nm, using a dual rf excitation diode.¹⁵ Films of Ta can be deposited in an α (bcc) phase or a β (tetragonal) phase, with respective bulk resistivities at 300 K of 13.4 and 160 $\mu\Omega$ -cm. The α is desirable because of its lower resistivity. Using Ar⁺ ions, an operating regime for depositing α -phase Ta was found at ion energies <20 eV and ion/atom ratios >13 for Si/SiO₂ substrates. The energy doses were typically several hundred eV/atom. A resistivity of 14.8 $\mu\Omega$ -cm was obtained at 5 eV and an ion/atom ratio of 23.

Using p-type (100) Si substrates, the minimum ion/atom ratio at 10 eV dropped from 13 to 10.5. Comparing Ar⁺ and Xe⁺ bombardment of Ta on a Si substrate at an ion/atom ratio of 25, a resistivity of about 25 $\mu\Omega$ -cm could be obtained at about 20 eV with Ar⁺ ions and at about 40 eV with Xe⁺ ions. From process comparisons with Ar⁺ and Xe⁺ ions, it was concluded that the formation of the α -Ta films was governed by ion momentum rather than energy.

2.3.2 111-textured titanium nitride - sputter deposited Ti. Sputtered Ti was deposited on a highly oriented 25-nm-thick 0002 Ti underlayer on a Si(001) substrate at a temperature of 450°C, with N₂⁺ ion bombardment to deposit dense TiN layers with a complete 111 texture.¹⁶ To obtain this texture, an ion/atom (N₂⁺ ions and the total of Ti and N atoms) ratio of

7 was used at a N_2^+ ion energy of about 20 eV, which corresponds to an energy dose of 140 eV/atom. The increased effectiveness of the 111 textured TiN as a barrier layer was demonstrated by depositing an overlayer of aluminum, and then determining the temperature at a constant ramp rate of 3°C/s at which interfacial Al_3Ti is observed. With the 111 texturing, the temperature reached 610°C before observing Al_3Ti , compared to 450°C with a conventional underdense layer of TiN with mixed 111/002 orientation.

3. LOW-ENERGY APPLICATIONS (~25-100 eV)

3.1 Cleaning - removal of physisorbed contamination

Film adhesion, purity, or some other property can benefit from removal of physisorbed contamination such as water, hydrocarbons, N_2 and O_2 . The low binding energy of this contamination to the surface, typically up to several tenths of an eV, can result in efficient removal of contamination. For example, vapor deposition of Nb on surfaces at $\leq 100^\circ C$ resulted in contamination by oxygen from the 10^{-8} Torr O_2 background pressure.³¹ Bombardment by 100 eV Ar ions removed the oxygen with the very high sputter yield of 40-50 O atoms/ion. For most cleaning applications, physisorbed contamination can be removed with ions having energies ≤ 100 eV. One should be aware, however, that special applications can require lower energies, with the extreme example of semiconductor cleaning given in Section 2.1 for GaAs. Because of the low binding energy of physisorbed contamination, the dose recommendations are based on covering the atomic deposition sites available, without regard to energy.

3.1.1 Initial cleaning. Using an approximate atomic dimension of 3 Å, there would be about 10^{15} atomic sites per cm^2 and an ion dose of 1.6×10^{-4} C/ cm^2 would provide one (singly-charged) ion per atomic site.²¹ This dose is recommended as the starting point for initial cleaning. It could be applied with various combinations of current densities and times, for example as 0.16 mA/ cm^2 for 1 s, or 1.6 $\mu A/cm^2$ for 100 s. This dose level is low enough that there should be little difficulty in reaching or exceeding it.

3.1.2 Continuous cleaning. If the contamination is continuously deposited from the vacuum-chamber background, then cleaning should remove this contamination as rapidly as it is deposited. For a background contamination of 10^{-6} Torr (1.3×10^{-4} Pa), a monolayer of contamination would be deposited in about one second. To remove this contamination as rapidly as it is deposited, an ion current of 0.16 mA/ cm^2 would be required. If the background contamination of interest were only 10^{-9} Torr (1.3×10^{-7} Pa), the required ion current would be 0.16 $\mu A/cm^2$.²¹

3.2 Metal and semiconductor films

Most metals and semiconductors can be deposited in dense, durable films with ion assist from ions in the low-energy range. While the effects of substrate temperature can be of theoretical interest, most practical interest is probably in films deposited at or near room temperature (approximately $\leq 100^\circ C$). This temperature limitation results from both the effects of relative thermal expansion and the possibility of high-temperature damage to either the substrate or to other components attached to the substrate.

Ion assist of metal films with low-energy ions (≤ 100 eV) is generally associated with large crystallite size. A sufficiently high film temperature will also increase crystallite size.^{18,32} Microhardness generally increases as crystallite size decreases.³² Because crystallite size does not vary rapidly in the low-energy range, the effects of ion assist on microhardness are moderate. Gas incorporation due to ion bombardment is low in the low-energy range.^{32,33} Argon appears to be deposited preferentially at grain boundaries, so that the low incorporation is probably a result of the large crystallite size in this energy range. Increasing the substrate temperature decreases the argon incorporation, due to both increasing crystallite size and increasing diffusion of argon.^{18,20}

Vapor deposited metal films usually show tensile stress when deposited on substrates at or near room temperature because of low adatom energy, with higher magnitudes of this stress typically shown by refractory metals.³⁴ This tensile stress is usually reduced by bombardment with ions having energies of ≤ 100 eV. A large enough ion-assist dose may, or may not, result in a compressive stress, but, for most single-component materials, any compressive stress would be small compared to the initial tensile stress for ≤ 100 eV ion assist. This effect of ion assist is in addition to any mismatch in thermal

expansion for films deposited at temperatures substantially different from room temperature. A reduced stress is one criterion for ion-assist effectiveness for a metal or semiconductor film. Another criterion is film density. The film density may be measured directly, or it may be measured through resistivity, with a near-bulk resistivity indicating a dense metal film. Because of the different properties of different materials, there is no single criterion for evaluating ion-assist effectiveness.

3.2.1 Copper. Films of Cu were vapor deposited with thicknesses of 5-6 μm at rates of 6-20 $\text{\AA}/\text{s}$ on Si and Si/SiO₂ substrates at 107°C, with ion assist provided by 62 eV Ar⁺ ions.³² Energy doses up to 18 eV/atom on Si substrates with various crystal orientations showed little effect on crystallite size (about 1000 \AA). This lack of effect of ion dose is in contrast to the substantial observed effect at higher ion energies (see Section 4.2.1). For Si/SiO₂ substrates, the microhardness dropped from 130 to 110 kg/mm² as the ion-assist dose increased from about 0 to 24 eV/atom. For Si(100) and Si(111) substrates, the microhardness increased from about 100 to 210 kg/mm² as the dose increased from near 0 to 25 eV/atom, showing in this case an effect of the substrate crystal structure on the microstructure of the film. The fraction of argon incorporated in these films was only a few tenths of a percent at 125 eV. From previous work, the incorporation at 62 eV was estimated at more than an order of magnitude lower at 62 eV.³² The resistivity increased from about 2.0 to 2.5 $\mu\Omega\text{-cm}$, generally increasing as the dose increased from near 0 to 24 eV/atom. The value of resistivity, together with the lack of any decrease as the dose increased, indicated a near-bulk density.

In a separate publication giving stresses, films of Cu were vapor deposited to thicknesses of 5 μm at rates of 5-20 $\text{\AA}/\text{s}$ on substrates at 107°C with assist provided by 62 eV Ar⁺.¹⁸ An initial tensile stress of more than 0.4 GPa, was reduced to zero stress at an ion/atom ratio of 0.03 and an energy dose of 2 eV/atom. A compressive stress of nearly 0.1 GPa was obtained with an increased ion/atom ratio of 0.08 and an energy dose of 5 eV/atom. Further increases of ion-assist doses up to 25 eV/atom reduced the compressive stress and, at the higher doses, gave a small tensile stress. From this study, an energy dose of about 3 eV/atom would be recommended to give near minimum stress at an Ar⁺ ion energy of 62 eV.

Optical characteristics were not found for Cu films in the low-energy regime, but can be inferred from high-energy studies ranging from 200-1000 eV (see Section 4.2.1).^{35,36} A study of vapor deposited Cu films on Cu substrates with Ar⁺ ion assist at an energy dose of 1.5 eV/atom showed that, over a range of 200 to 1000 eV, the roughness increased with energy, indicating that the optimum ion energy would be less than 200 eV.

3.2.2 Germanium. Films of Ge were vapor deposited with 100-350 eV Ar⁺ ion assist at ion/atom ratios from 0 to 1.³⁷ The 100 eV data are pertinent here. In general, the optimum dose was an ion/atom ratio of 0.005-0.007 with 100 eV ions, or 0.5-0.7 eV/atom. The optical bandgap was a minimum of 0.74 eV with an ion/atom ratio of 0.007 of 100 eV ions, which compares to a bandgap of 0.67 eV for crystalline Ge. The minimum resistivity corresponded to the minimum in the optical bandgap. Hall measurements showed a maximum electron mobility of 700 cm²/V-s at an ion/atom ratio of 0.005 with 100 eV ions, or a dose of 0.5 eV/atom. The polarity of the measurements corresponded to n-type semiconductors. The grain sizes remained at several hundred \AA , regardless of ion-assist dose. The small ion-assist dose (0.5-0.7 eV) together with the lack of structural changes (constant grain size) indicate that the process is more in the nature of cleaning (removing contamination) than it is in changing the properties of the deposited material. For comparison, see Section 3.2.4 - Nb. No conclusion is reached from this study regarding an optimum ion-assist dose for Ge.

In another study, films of Ge 2 μm thick were deposited at a rate of 2.2 $\text{\AA}/\text{s}$ on unheated glass substrates, with ion assist provided by Ar⁺ ions at energies of 65-3000 eV.³⁸ The ion/atom ratio to assure adherence of the film to the substrate was determined over the energy range. Although the stress was not directly measured, a barrier layer of Ge 100 nm thick was deposited without ion assist to prevent an improved interfacial bond with the glass from affecting the adherence. At 65 and 100 eV, the ion/atom ratios for good adherence were about 0.09 and 0.035, while the energy doses were about 6 and 3.5 eV/atom. The incorporation of Ar was not detectable at or below 100 eV.

A thorough study of Ge density has been made in the low-energy regime.⁶ Films of Ge were vapor deposited to thicknesses of 200-300 nm at rates of 3-8 $\text{\AA}/\text{s}$, with ion assist provided by Ar⁺ ions at 15-110 eV. The ion/atom ratios of 15 eV ions were not sufficient to reach minimum void fraction. Ions of 30, 50, 70, 90, and 110 eV all reached minimum void

fraction at energy doses of 4.5-5.5 eV/atom. The significance of this study is in the degree of correlation demonstrated when the results with different energies are compared on an eV/atom basis.

3.2.3 Gold - O_2^+ ions. Optical films of Au were vapor deposited at a rate of 5 Å/s on unheated alumina substrates with ion assist by 100 eV O_2^+ ions.³⁹ Using an ion/atom ratio of 0.42-0.63 and a dose of 42-63 eV/atom, films had good adhesion and nominal reflection. To obtain good adhesion for gold on oxide substrates without ion assist, it is common to use a transitional or "glue" layer between the substrate and the gold.⁴⁰ The transitional layer can be a couple of hundred angstroms of Cr vapor deposited in a low- 10^{-2} Pa background of O_2 . The use of ion assist with O_2^+ ions avoids the need for this transitional layer.

3.2.4 Niobium. An Ar^+ ion energy of 100 eV and substrate temperatures from 100-400°C showed a consistent pattern of crystallite size increasing with ion-assist dose and substrate temperature. The complete range in crystallite size was about 90-250 Å.¹⁸ Only relative dose levels were given.

In another study, films of Nb were vapor deposited on Si substrates to a thickness of about 200 nm at a rate of 4 Å/s, with ion assist provided by Ar^+ ions at 100 eV.³¹ With substrate temperatures <100°C, the films were found to have compressive stress, which was due to contamination from a 10^{-8} Torr background of O_2 . An ion-assist dose of 9.4 eV/atom was sufficient to remove most of this contamination at a substrate temperature of 100°C, which also resulted in a change from compressive to a tensile stress of 0.7-0.8 GPa. Higher substrate temperatures resulted in lower oxygen contamination, a shift toward tensile stress, and a reduction in the ion-assist dose required to reach a tensile stress of 0.7-0.8 GPa. At 400°C, the O_2 contamination was reduced sufficiently so that no ion assist was required to reach a tensile stress of 0.7-0.8 GPa. The calculated sputter yields of 40-50 for O atoms/ion indicate that the oxygen was physisorbed rather than chemisorbed. This discussion is included to show the effect contamination can have on film stress. Resistivity was reduced to near the bulk value during the removal of contamination, indicating a near-bulk density was reached before the ion assist started to reduce the customary tensile stress.

After the removal of oxygen contamination, as described above, additional ion assist at 100 eV reduced the tensile stress. An ion/atom ratio of 0.05 and an energy dose of 5 eV/atom was sufficient to remove most of this tensile stress from a film deposited at 400°C. The range of the data was not large enough to show the dose required to remove most of the stress in a film deposited at 150°C, but extrapolation of the trend indicated a dose of about 25 eV/atom. In the absence of contamination, 25 eV/atom would be the recommended ion-assist energy dose.

3.2.5 Silver - O_2^+ ions. Films of Ag were vapor deposited at a rate of 5 Å/s on unheated substrates and were ion assisted with an O_2^+ ion beam.³⁹ Using 120 eV O_2^+ ions, an ion/atom ratio of 0.85, and a dose of 102 eV/atom, the films incorporated 8 percent oxygen and had poor reflectivity (the desired property). Dropping the O_2^+ ion energy to 100 eV and using an ion atom ratio of 0.43 for a dose of 43 eV/atom, the film adhered well on unheated glass substrates and was highly reflecting. This use of O_2^+ ion assist may improve adhesion for Ag films on oxide substrates, similar to the use of O_2^+ ion assist on Au (see Section 3.2.3).

3.2.6 Tungsten. The incorporation of Ar, Kr, Ne, and Xe in tungsten was investigated.³³ The incorporation of all of these gases increased rapidly with ion energy. With the exception of Ne, which was incorporated at several percent, all of these gases had about 1 percent or lower incorporation at an ion energy of 100 eV.

In another study, films of W, 200 nm thick, were sputter deposited in a dual ion beam system using Ar^+ ion sputtering energies of 400, 600, and 1200 eV and ion/atom ratios of 0-0.038 with an Ar^+ ion-assist energy of 100 eV.⁴¹ The stress remained compressive at all times. The variation in stress for different sputtering ion energies (higher compressive stress for higher energy) was roughly as large as the effect of ion assist. It was concluded that reflected argon from the target had a significant effect. With the atomic mass of W more than four times that of Ar, energetic Ar atoms (from beam ions) could be reflected with minimal energy loss. The 100-eV ion assist had an "annealing" effect, in that the magnitude of the compressive stress was reduced, but an ion-assist dose cannot be recommended because the ion-assist effect could not be

separated from the effect of energetic neutrals. These results are included herein to show the effect reflected energetic neutrals can have on film stress.

3.2.7 Tungsten silicide. WSi_2 was vapor deposited from separate W and Si e-gun evaporators on Si substrates at room temperature, with Ar^+ ion assist at 100 eV and eV/atom ratios of 0-6.4.⁴² The stress without ion assist was tensile, 0.5-0.6 GPa, dropped to zero at a dose of about 5 eV/atom, and became compressive, 0.1 GPa, at the maximum dose of 6.4 eV/atom. If the WSi_2 was to be used in the as-deposited state, with room-temperature deposition, an ion/atom ratio of 0.05 and an energy dose of 5 eV/atom would be recommended. However, the resistivity of the WSi_2 films dropped by about a factor of ten when subjected to a post-deposition anneal at 1000°C, and the stress after anneal was not significantly affected by the ion assist during deposition.

3.3 Oxide, nitride, and fluoride films

Many compounds can be deposited in dense, durable films without ion assist, if the substrate temperature is high enough.⁴³ In many cases, the difference in thermal-expansion coefficients between the film and substrate make high substrate temperatures impractical. When multiple layers of different film materials are involved, it becomes more unlikely that high substrate temperatures can be used. What ion-assisted deposition offers is a film quality similar to that obtained with high substrate temperature, but with a moderate substrate temperature.

Oxide, nitride, and fluoride films are compounds of solid and gaseous elements. There are several options for their deposition. The compound can be deposited directly, or deposited as the solid element (e.g. Al or Si) and reacted with the gaseous element (e.g., N_2 or O_2) as it is deposited. The deposition reaction can, in turn, be direct with ions of the gaseous element or indirect with inert-gas ions activating the reaction with adsorbed gas from the background. The most common options are to vapor deposit either the solid element or the compound, with ion assist using ions of the gaseous element.

Maintaining stoichiometry is a basic requirement in compound deposition. Ion bombardment of the compound sputters away both the solid and gaseous elements, but removes the gaseous element more rapidly. Considering only the sputtering process, this would leave the surface of a compound with an over-stoichiometric fraction of the solid element. The reduced sticking coefficient or reacting coefficient of excess energetic gaseous molecules can be used to offset the preferential sputtering. See, for example, Section 3.4.1 - AlN. The practical solution usually involves an excess of the gaseous molecules, either as ions or background gas, to assure stoichiometry.

Obtaining a dense dielectric structure without excess damage from energetic ions is another basic requirement. In the absence of ion bombardment, many compounds are deposited on low-temperature substrates in a shadowed columnar form, corresponding to Zone 1 of the Thornton zonal model.^{10,43} This structure is porous and is susceptible to degradation and shifts in film properties when exposed to moisture. Sufficient ion assist will compact this structure into a dense polycrystalline or amorphous structure that is much more resistant to the effects of moisture. However, if the ion assist involves excessively energetic ions, the film properties can be degraded by damage sites and implanted ions. The practical solution usually involves using low ion energies where implantation and defects are unlikely. If the ion energies are ≤ 100 eV, moderate excesses in doses usually have few adverse effects. Several of the following examples use an ion energy of 120 eV. Despite energies slightly over the nominal limit of 100 eV, these examples are believed to belong more to the low-energy regime than the high-energy regime.

3.3.1 Aluminum nitride - sputter deposited Al. A dual ion beam system was used to deposit AlN, with the Al sputter deposited by a 1500 eV Ar^+ ion beam from one ion source and reactive ion assist provided by a 100-500 eV N_2^+ ion beam from the other ion source.⁴⁴⁻⁴⁶ The results with 100 eV Ar^+ ions are pertinent here. Ion bombardment by N_2^+ ions up to arrival ratios needed to form AlN were almost fully incorporated into the Al films. Excess N_2^+ ions above the value needed to form AlN were rejected, resulting in AlN films when that excess was provided. When insufficient N_2^+ ions were provided, AlN grains were formed in an Al matrix. When the ion-assist ion source was turned off, but N_2 was present in the background, no AlN grains were formed, even though 9 percent N was present in solution in the Al. There may have been reflected neutrals from the 1500 eV bombardment of the Al target (see Section 3.2.6 - W), but the absence of AlN grains without ion assist showed that these energetic neutrals did not have a significant effect on the formation of AlN as

described above. This example is included to show the variation in incorporation of the nitrogen ions to maintain stoichiometry. Without stress, adhesion, or density measurements, no ion-assist dose can be recommended.

3.3.2 Aluminum nitride - vapor deposited Al. Vapor deposited Al was used to grow AlN films of 150-200 nm thick on Si(111) and silicate glass substrates.⁴⁷ For a film deposited at 2.5 Å/s, with N₂⁺ ion assist at 60 eV, Stoichiometry was obtained at N/Al arrival rates of 1.5 or more. This implies a sticking coefficient at the 1.5 arrival rate of about 0.7, compared with near unity for sputter deposited Al in the preceding section.

3.3.3 Aluminum oxide. Vapor deposited Al was used to grow Al₂O₃ films 2.1 μm thick at a rate of 13 Å/s on unheated substrates, with ion assist provided by O₂⁺ ions at 120 eV.³⁹ The refractive index was homogeneous at 1.65, with no observed absorption. An SEM micrograph showed morphology that corresponded to between Zone II and Zone III of the Thornton zonal model,^{10,43} which would be expected to provide resistance to the effects of moisture. The ion/atom (O₂⁺ ions and total deposited atoms) ratio was 0.17 with a dose of 20 eV/atom.

3.3.4 Cerium oxide. Vapor deposited Ce was used to grow CeO₂ films with ion assist provided by O₂⁺ ions at 120 eV.³⁹ To increase film density, the deposition rate had to be less than about 1.2 Å/s on unheated substrates. The refractive index was 2.35 on unheated substrates (2.4 on 300°C substrates). The ion/atom ratio was 3.62 with a dose of 430 eV/atom at the 1.2 Å/s deposition rate.

3.3.5 Hafnium oxide. Vapor deposited Hf at 3 Å/s was used to grow HfO₂ films at a rate of about 5 Å/s on unheated substrates with ion assist provided by 120-eV O₂⁺ ions in an O₂ background at 10⁻² Pa.³⁹ The films were optically homogeneous and showed no vacuum-to-air spectral shift. The ion/atom ratio was 0.62 with a dose of 74 eV/atom.

3.3.6 ITO. Indium tin oxide was vapor deposited on polycarbonate substrates from In and ITO bulk (90% In₂O₃, 10% SnO₂, both by weight) to a thickness of 85-95 nm at a rate of 0.3 Å/s, with ion assist from O₂⁺ ions at 60 eV. Oxygen background pressure was maintained at 0.011 Pa.⁴⁸ Low resistivity (4.1×10⁻⁴ μ-cm) and high transmittance (~80%) in the visible range were obtained with an ion/atom ratio of about 0.4, an energy dose of less than 3 eV/atom, and a substrate temperature of 50°C. (An ion/atom ratio of 1.0 is given in the paper, but other numbers therein indicate that this ratio is based on metal atoms.) Adhesion was improved by an Ar⁺ ion dose of 1×10¹⁶ ions/cm² on the polycarbonate substrate before deposition, with the total Ar and O₂ background pressure <0.027 Pa.

In another study, indium tin oxide was vapor deposited with low-energy ion assist at both 100 and 300°C substrate temperatures.³⁹ At 300°C, a ratio of 80% In and 20% Sn by weight was vaporized at a rate of 10 Å/s and deposited with O₂⁺ assist to give a sheet resistance of 20 Ω/sq, a refractive index of 2.0 (550nm), and a transmittance of 85% (550 nm) for a thickness of 350 nm. To achieve the same resistance and transmittance at 100°C, the ratio of In and Sn had to be reversed and the evaporation rate reduced by a factor of two. Information included was insufficient to calculate ion/atom ratios and energy doses.

3.3.7 Magnesium fluoride. Vapor deposited MgF₂ was used to grow MgF₂ films on unheated substrates with ion assist by Ar⁺ ions at 120 eV and O₂⁺ ions at 100 eV.³⁹ Ion/atom ratios and doses were not available, but assisted deposition with Ar⁺ ions resulted in a refractive index of 1.39 and less than 0.005 absorption. The use of O₂⁺ ions resulted in a refractive index of 1.39 and less than 0.001 absorption. The films adhered well, but were less durable in a rub test than films deposited without ion assist on substrates heated to 350°C. The high absorption compared to that of other ion-assisted optical films described herein is probably the result of the preferential loss of F during ion bombardment. The improvement with O₂⁺ over Ar⁺ bombardment may be due to the oxidation of excess Mg to MgO.

3.3.8 Silicon dioxide. Vapor deposited Si and SiO were used to grow SiO₂ films on unheated substrates with ion assist provided by 90 eV O₂⁺ ions.^{39,49} Starting with Si, SiO₂ films were deposited at 10 Å/s with an ion/atom ratio of 0.13 and a dose of 11 eV/atom. The refractive index was 1.48 at 550 nm. Adhesion and abrasion resistance were excellent. There was less inhomogeneity and adsorption when the deposition rate was reduced to 3 Å/s. Starting with SiO, SiO₂ films were deposited at 10 Å/s with an ion/atom ratio of 0.09 and a dose of 8 eV/atom. There was also an O₂ background of 0.02 Pa.

The refractive index was 1.468 at 550 nm. The adsorption was below the threshold for the simple measurement technique used. The films showed good homogeneity and passed adhesion and abrasion resistance tests. The SiO₂ film stress was compressive, 0.2 GPa (a good match in multilayer filters for ion-assisted TiO₂ with a tensile stress of 0.2 GPa). It was necessary to use end-Hall ion-source characteristics⁷ and the geometry of the vacuum chamber⁴⁹ to estimate the ion/atom ratios and the ion energies.

3.3.9 Tantalum oxide. Vapor deposited Ta₂O₅ was used to grow Ta₂O₅ films at 5 Å/s with ion assist provided by either 100 or 1000 eV O₂ ions and an O₂ background of 0.005 Pa.⁵⁰ The ion assist with 100 eV O₂ ions is pertinent here. Without ion assist, the refractive index at 633 nm was 1.93, but increased to 2.14 with an ion/atom ratio of 0.19 and an energy dose of 19 eV/atom. The extinction coefficient ranged from 3-4×10⁻⁴. (It was more than a factor of ten higher for ion assist at 1000 eV.) Based on the optical qualities, 19 eV/atom is the recommended ion-assist dose. Without ion assist, the film stress was tensile, about 0.1 GPa, but changed to neutral with an ion/atom ratio of about 0.04, and was a maximum compressive stress of 0.4 GPa for an ion/atom ratio of 0.3. The microhardness increased from about 7 GPa with no ion assist to about 10 GPa for ion atom ratios of 0.08 or higher.

3.3.10 Titanium dioxide. Vapor deposited TiO₂ was used to grow TiO₂ films at 4 Å/s with ion assist provided by 90 eV O₂⁺ ions on unheated glass substrates.^{39,49} The ion/atom ratio was 0.26 and the dose was 23 eV/atom. The refractive index was 2.43±0.02 and the extinction coefficient was at least in the low 10⁻⁴ range, both at 550 nm. The stress is tensile at 0.2 GPa and the films have excellent adhesion and good abrasion resistance. It was necessary to use end-Hall ion-source characteristics⁷ and the geometry of the vacuum chamber⁴⁹ to estimate the ion/atom ratios and the ion energies.

3.3.11 Yttrium oxide. Vapor deposited Y was used to grow Y₂O₃ films at 3.4 Å/s with ion assist provided by 120 eV O₂⁺ ions on unheated substrates.³⁹ Excellent antireflective coatings were deposited on temperature sensitive substrates. The ion/atom ratio was 1.08 and the dose was 130 eV/atom. The range of refractive index was 1.8-1.85, which was substantially reduced from deposition without ion assist. No oxygen background was required for stoichiometry.

3.3.12 Zirconium dioxide. Vapor deposited Zr was used to grow ZrO₂ films at 4.5 Å/s on unheated substrates with ion assist provided by 120 eV O₂⁺ ions with an O₂ background pressure of 10⁻² Pa.³⁹ Compared to ion assist at higher energies, excellent films were obtained with a high refractive index and low absorption. The ion/atom ratio was 0.65 and the dose was 78 eV/atom.

3.4 Summary of low-energy films

The Thornton zonal model⁴³ gives film microstructure from sputter deposition as a function of substrate-to-melting temperature ratio, T_s/T_m , and Ar pressure. At low values of T_s/T_m , the film has poor mechanical integrity. It is also porous so that moisture can propagate through the film with resulting adverse effects. The effect of Ar pressure can be interpreted as being due to trapping of Ar.¹⁰ We prefer the interpretation that the Ar pressure affects the energy of the sputtered particles,⁵¹ so the Ar variation can be replaced with a corresponding variation in ion-assist energy.⁵² We propose further that, for the low-energy regime where ion-assist processes appear to be dominated by lattice vibrations, that the required ion-assist energy dose (eV/atom) might be a function of the temperature ratio, T_s/T_m . Because the substrates are all at low temperature (approximately ≤100°C), there is no need to plot against temperature ratio. In Fig. 2, most of the recommended energy doses herein are plotted against T_m . Included are recommended doses for films of Cu, Ge, Nb, (all assisted with Ar⁺) and Al₂O₃, CeO₂, HfO₂, SiO₂, Ta₂O₅, TiO₂, Y₂O₃, and ZrO₂ (all assisted with O₂⁺). The films that were omitted were WSi₂ (the appropriate melting temperature is not clear when it undergoes a crystallization at an anneal temperature of 1000°C), Ag and Au deposited with O₂⁺ ions (the appropriate melting temperature is not clear when the process involves both a metal film and the interaction of O₂⁺ ions with an oxide substrate), and ITO (because In₂O₃ volatilizes before it melts). The plot shows a clear trend from under 10 eV/atom for materials with low melting temperatures to 100 eV/atom or more for materials with higher melting temperatures. Figure 2 is suggested for estimating energy doses for new applications in the low-energy regime.

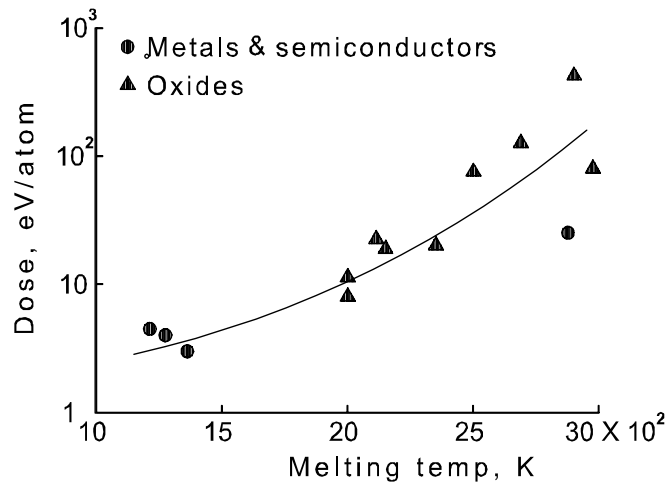


Fig. 2. Ion-assist energy dose for low-energy applications at low substrate temperatures (approximately ≤ 100 eV).

3.5 Metastable states

Copper was vapor deposited with ion assist by O_2^+ ions with an energy of 100 eV.²⁰ The O/Cu arrival ratio, with the O from O_2^+ , was varied from 0.1 to 3.1. The O_2 background pressure was varied from about 0.007-0.09 Pa. For O/Cu ratios from about 0.2 to 0.5, Cu_2O was deposited. From >0.5 to about 0.8, Cu_5O_4 was deposited. From about 1.0 and greater, CuO was deposited. The Cu_5O_4 deposit was determined to be a metastable polycrystalline compound. In the absence of an ion beam, less than 2 percent oxygen was incorporated in the film. (This investigation was actually carried out by C.R. Guarneri, but has only been reported elsewhere.⁵³)

4. HIGH-ENERGY APPLICATIONS (100-1000 eV)

4.1 Cleaning - removal of chemisorbed contamination

Film adhesion, purity, or some other property can benefit from removal of chemisorbed contamination such as oxides, nitrides, or some other compounds. The binding energy of chemisorbed contamination to the surface is typically several eV and its removal is a sputtering process. Because of the energies involved, there is usually no sharp distinction between removing a chemisorbed contamination on the surface and removal of some of the material beneath the surface.

The removal of chemisorbed contamination is a high-energy process in that it generally increases with increasing energy over the range 100 to 1000 eV covered in this section. Ion energies of several hundred eV can be used with tables of sputter yields⁵⁴ to calculate the cleaning dose required. For many cleaning applications, however, chemisorbed contamination can also be removed with ions having energies ~ 100 eV to minimize damage to the material beneath the surface. Some low-energy sputter yields are available.

4.1.1 Copper oxide. The atomic sputter yield of oxygen from a saturated oxidized surface of copper rises from a threshold at about 30 eV to reach unity below 100 eV. The sputter yield would be expected to drop as the coverage of oxygen decreases. As a limiting case, the sputter threshold for Cu is about 25 eV and the yield is about 0.4 at 100 eV.¹¹ Oxygen is preferentially sputtered to a higher degree from oxides with a low bond energy (e.g. Cu-O) relative to those with a high bond energy (e.g. Si-O).

4.1.2 Silicon. The sputter yield of Si to bombardment by Ar^+ ions increases linearly from near zero at about 40 eV to 0.2 at 100 eV.⁵⁵

4.1.3 Silicon dioxide. The sputter yield of SiO_2 to bombardment by Ar^+ ions increases linearly from near zero at about 50 eV to 0.5 at 300 eV. The sputter yield at 100 eV is about 0.1.⁵⁵

4.2 Metal and semiconductor films

Most metals and semiconductors can be deposited in dense films with ion assist from ions in the high-energy range. As the energy is increased within this range, however, there is an increasing price in increased defect density and increased incorporation of the working gas.¹³ Some of the adverse effects of high ion energy can be offset by depositing on a heated substrate, or by a post-deposition anneal. There can be an upper limit on assist ion energy, where the assist ions remove atoms by sputtering as rapidly as they are deposited.¹¹ As in the low-energy regime, reduced stress and increased film density are criteria for evaluating the effectiveness of ion assist for a metal or semiconductor film. Again, because of the different properties of different materials, there is no single criterion for evaluating ion assist. The effects of ion-assist on stress, in particular, vary with the material.

4.2.1 Copper. Films of Cu were deposited with thicknesses of 5-6 μm with ion assist by Ar^+ ions.¹⁸ An ion energy of 125 eV at 82°C did not show much difference in crystallite size from that found at 100 eV and 107°C. An ion energy of 600 eV and temperatures of 103° or less resulted in approximately half the crystallite size compared to 62 eV and 125 eV. At 600 eV, the crystallite size dropped from about 600 Å at about 1 eV/atom to 250-300 Å for the range of 10-39 eV/atom. Increasing the substrate temperature to 230°C at 600 eV increased the crystallite size by about 100 Å over the ion-assist dose range investigated. The asymptotic microhardness (250-300 Kg/mm²) was over twice the untreated value at an Ar ion energy of 600 eV, and required a dose of about 30 eV/atom to reach. The asymptotic value was lower at 125 eV, 250-300 Kg/mm², but only required doses of the order of 3 eV/atom to reach. The resistivity at 125 eV and 80°C increased from about 2.0 to 2.7 $\mu\Omega\text{-cm}$ as the dose increased from near 0 to 45 eV/atom, with most of the increase between 0 and 10 eV. The resistivity at 600 eV and 62-103°C increased from about 5 to 12 $\mu\Omega\text{-cm}$ as the dose increased from near 0 to 35 eV/atom. With 600 eV and 230°C, the resistivity ranged from about 2 to 8 $\mu\Omega\text{-cm}$ with doses from near 0 to over 100 eV/atom.

An initial tensile stress of more than 0.4 GPa was reduced to a zero tensile stress by an ion-assist dose of 15-20 eV/atom using 600 eV ions, and to a compressive stress of nearly 0.1 GPa by an ion-assist dose of 30-35 eV/atom. On the basis of stress an ion/atom ratio of 0.025-0.033 and an energy dose of 15-20 eV/atom would be recommended. There was excellent agreement for ion assist at 62 and 600 eV, when stresses were plotted against ion/atom ratio. This means that it took almost ten times the energy dose in eV/atom to produce the same effect at 600 eV as it did at 62 eV.

In a separate study, the optical-scatter characteristics of vapor deposited Cu films grown at a rate of 3 Å/s with Ar^+ ion assist at 300 eV were investigated.^{35,36} Starting with a polished Cu surface of 33.5 Å rms roughness, the roughness was reduced to 26.9 Å by a 200 nm Cu film without ion assist, or alternatively reduced to 15.75 Å by a 200 nm Cu film with ion assist at an ion atom ratio of 0.0074 and an energy dose of 2.2 eV/atom. Sputter deposited Cu films showed a roughness intermediate of vapor deposited Cu films with and without Ar^+ ion assist. Other tests investigated other parameters and similar improvements were found with other substrates; the roughness decreased with increasing thickness of the Cu film up to the maximum investigated of 1000 nm; and the roughness further decreased with an increase in ion assist to 0.025 ion/atom and 7.4 eV/atom. Reflectivity also increased with ion assist, 5-10 percent over the visible spectrum when compared to a vapor deposited Cu without ion assist. A series of samples was also made with the ion/atom ratio varied to maintain the energy dose at 1.5 eV/atom while varying the ion energy from 200 to 1000 eV. This series showed that the roughness increased with increasing ion energy. As a general conclusion of this investigation, the deposition of vapor deposited Cu films resulted in a reduction of optical scatter, but this reduction was not reflected in mechanical (Talystep) measurements of surface roughness.

4.2.2 Germanium. Films of vapor deposited Ge were deposited on unheated glass substrates and ion assisted at Ar^+ energies of 65-3000 eV.³⁸ Ion assist doses to assure adhesion were evaluated over the ion energy range. Stress was not measured directly, but reduced stress is assumed to be the cause of the better adhesion. The required ion/atom ratio was found to vary as $\text{eV}^{-3/2}$. At 100 eV, the ion atom ratio was 0.035 and the energy dose was 3.5 eV/atom. Interpolating the results for 1000 eV, the ion/atom ratio would be roughly 0.001 and the energy dose about 1 eV/atom. Comparison of this variation in ion-assist dose with energy with that of Cu in the preceding section will show the difficulty of including both stress variations with energy in one theoretical description.

4.2.3 Tungsten silicide. WSi_2 was deposited from separate W and Si e-gun evaporators on Si substrates, with ion assist at 400 eV and ion/atom ratios of 0-0.06.⁴² The resistivity with room temperature deposition varied over the range from 550 to 620 $\mu\Omega\text{-cm}$ for this ion/atom range. This variation did not differ greatly from that with 100 eV ions. Because WSi_2 is not a simple element, other factors are likely to be involved. As an example, still using 400 eV ions, but increasing the substrate temperature to either 350 or 500°C resulted in roughly doubling the resistivity over the same ion-assist dose range. The stress without ion assist was tensile, 0.5-0.6 GPa, dropped to zero at a dose of about 12 eV/atom, and became compressive, nearly 0.2 GPa, at the maximum dose of 25 eV/atom. On the basis of stress, an ion/atom ratio of 0.03 and an energy dose of 12 eV/atom are recommended at an ion energy of 400 eV. Comparing these results and the low-energy ones of Ge in Section 3.2.2 to the preceding results for Cu and Ge, Ge shows an ion energy effect intermediate of Cu and Ge. As mentioned in Section 3.2.7, a post-deposition anneal at 1000°C results in a major change in WSi_2 properties.

4.2.4 Other metals. As part of the investigation of the optical-scatter characteristics described in Section 4.2.1 for vapor deposited Cu films, the optical-scatter characteristics of sputtered Ag, Al, and Mo films were also investigated.³⁶ The improvements were similar to those described for Cu, but the ion-assist doses were not given.

4.2.5 Gas incorporation. Gas incorporation due to ion bombardment rises rapidly in the high-energy range,³³ and has been found to increase linearly with ion flux.⁵⁶ Amorphous metal films can contain large fractions of inert gas atoms under ion-assisted growth conditions, since they can have a wide range of interstitial volumes. Incorporated atomic fractions exceeding 0.4 have been observed for amorphous metal alloys of Gd, Co, and Mo, using 500 eV Ar^+ ions.⁵⁶

4.3 Oxide films

Historically, many ion-assisted deposition applications for oxide films were developed with gridded ion sources, with which it is difficult to obtain high processing rates without also using high ion energies. The publications typically describe results with a range of ion energies, often being limited in ion/atom ratios and energy doses at the lower ion energies. The end result was often the use of a compromise energy that was high enough to permit reasonable production rates without, at the same time, causing excessive damage. Many of these early compromise solutions satisfy their requirements quite well. On the other hand, for low film damage at low substrate temperature in a new application, the investigation should probably focus on the low-energy regime.

4.3.1 Aluminum oxide. Vapor deposited Al_2O_3 was used to grow 250 nm films of Al_2O_3 films at about 3 Å/s on high-index flint glass at about 100°C, with ion assist provided by O_2^+ ions at 150, 300, and 600 eV.^{57,58} The experimental results are shown in Fig 3(a) against ion/atom ratio (O_2^+ ions and total deposited atoms). The maximum ion/atom ratio was sufficient to reach a maximum refractive index (1.70-1.72, 350 nm) at 300 and 600 eV, but not at 150 eV. The extinction coefficient of Al_2O_3 is typically low, about 3×10^{-4} , without ion assist, and is further reduced by O_2^+ ion assist in the high-energy range. This coefficient does *not* increase at high ion/atom ratios as described in Section 4.3.4 for Ta_2O_5 . Tested as an $\text{Al}_2\text{O}_3/\text{SiO}_2$ antireflective coating, 300 eV ion assist greatly reduced moisture absorption and increased abrasion resistance (more abrasion resistance than $\text{Ta}_2\text{O}_5/\text{SiO}_2$ and $\text{TiO}_2/\text{SiO}_2$ antireflective coatings tested at the same time).

4.3.2 Cerium oxide. Vapor deposited CeO_2 was used to grow CeO_2 films of a thickness of 250-350 nm at a rate of 2.5-3 Å on fused silica substrates, with ion assist provided by O_2^+ ions or mixtures of O_2^+ and Ar^+ ions at 300-700 eV.⁵⁹ (From a description in another publication,⁶⁰ these substrates were unheated.) Without ion assist, the vapor deposited CeO_2 had a refractive index of 1.99-1.86, as the O_2 background pressure increased from $1-10 \times 10^{-3}$ Pa. With O_2^+ ion assist, the best properties were found at 600 eV with an ion/atom ratio of 0.61-0.73 and a dose of 370-440 eV/atom (the ranges are for the uncertainty of deposition rate). The refractive index was a maximum (2.3) with this ion assist and the extinction coefficient was $< 10^{-4}$. The films deposited at 700 eV showed an extinction coefficient of about 0.01. From the variation in refractive index with ion/atom ratio, the films at all ion assist energies ≤ 600 eV would have benefitted from higher ion/atom ratios than were investigated. For example, the 300 eV data had the same ion/atom ratio, so the dose was only 180-220 eV/atom. In other words, if higher ion/atom ratios had been investigated, lower ion energies might have been preferable.

In another publication, vapor deposited CeO_2 was used to grow CeO_2 films of a thickness of 225 nm at a rate of about 3 Å on fused silica substrates at temperatures from ambient (about 30°C) to 300°C, with ion assist provided by Ar^+ ions at 300-700 eV.⁶⁰ With Ar^+ ion assist, the maximum refractive index of 2.32 (550 nm) was found at 600 eV with an ion/atom ratio of 0.98 (the highest tested) and a dose of 590 eV/atom. The extinction coefficient was a minimum of about 0.02 at this condition and increased for lower ion/atom ratios or higher ion energies. The packing density was a maximum of about 0.9 at this condition and decreased for lower ion/atom ratios or either higher or lower ion energies. Comparison with O_2^+ ion assist above shows that the use of Ar^+ ion assist results in a higher extinction coefficient.

4.3.3 Silicon dioxide. Vapor deposited SiO_2 was used to grow SiO_2 films at 3 Å/s on high-index flint glass at about 100°C, with ion assist provided by O_2^+ ions at 300 eV.⁵⁸ With ion/atom ratios from 0 to 0.53, the refractive index increased slightly from 1.42 to 1.44 (350 nm), and the extinction coefficient remained about 2×10^{-4} regardless of dose. However, moisture absorption was greatly reduced by ion assist.

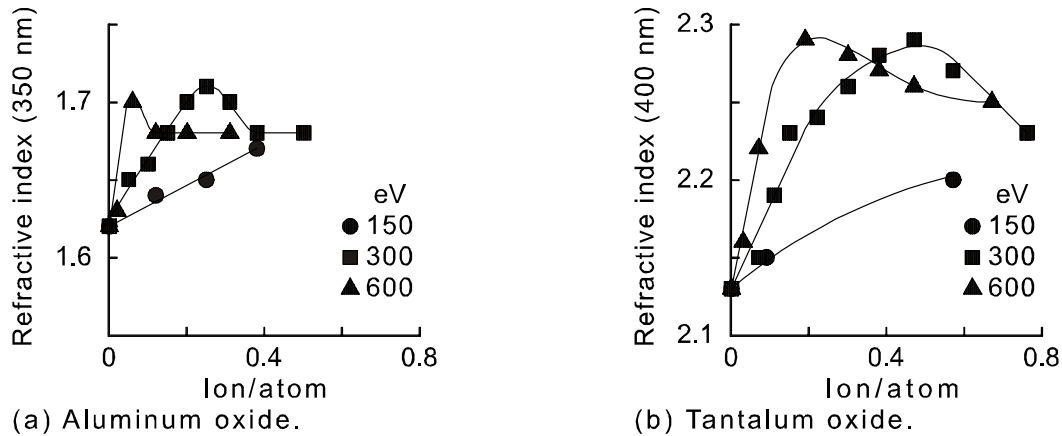


Fig. 3. Variation of refractive index with ion/atom ratio and ion energy in the high-energy regime.⁵⁸

4.3.4 Tantalum oxide. Vapor deposited Ta_2O_5 was used to grow Ta_2O_5 films at 5 Å/s with ion assist provided by either 100 or 1000 eV O_2 ions and an O_2 background of 0.005 Pa.⁵⁰ The ion assist with 1000 eV O_2 ions is pertinent here. Without ion assist, the refractive index at 633 nm was 1.93, but increased to 2.14 (the same as at 100 eV) with an ion/atom ratio of 0.05 and an energy dose of 50 eV/atom. The extinction coefficient ranged from 0.003 to 0.02, more than a factor of ten higher than for ion assist at 100 eV. Based on the optical qualities, the recommendation would be to use ion assist at 100 eV. Without ion assist, the film stress was tensile, about 0.1 GPa, but changed to neutral with an ion/atom ratio of about 0.04, about the same ratio as for 100 eV.

In another study, vapor deposited Ta_2O_5 was used to grow Ta_2O_5 films, 350 nm thick, at about 2 Å/s on fused-silica substrates at about 100°C using O_2^+ assist ions at 150, 300, and 600 eV.^{57,58} The experimental results are shown in Fig. 3(b). The ion/atom ratio was sufficient to reach a maximum refractive index (2.29, 400 nm) at 300 and 600 eV, but not at 150 eV. The maximum value reached at 300 and 600 eV is approximately the bulk value of refractive index, and is followed by a decrease at higher ion/atom ratios. The decrease at higher ion/atom ratios is believed to be due to excessive damage and gas implantation. The extinction coefficient at low substrate temperature is about 15×10^{-4} without ion assist, and drops to $< 2 \times 10^{-4}$ for low levels of ion/atom ratio. Further increases in ion/atom ratio near the maximum refractive index result in a subsequent increase in extinction coefficient. A comparison of ion assist at different substrate temperatures shows that the ion/atom ratio to reach maximum refractive index at 300°C is only about 30 percent of what is required at 100°C. Tested as an $\text{Ta}_2\text{O}_5/\text{SiO}_2$ antireflective coating, enough 300 eV ion assist to give near maximum refractive index resulted in substantially reduced moisture absorption and increased abrasion resistance.

4.3.5 Titanium dioxide. Vapor deposited TiO_2 was used to grow TiO_2 films, 250 nm thick, deposited at about 3 Å/s on fused-silica substrates at about 100°C, with ion assist provided by O_2^+ ions at 300 eV.^{57,58} The extinction coefficient of

TiO₂ is typically about 4×10^{-4} , regardless of O⁺ ion assist dose. This coefficient does *not* increase at high ion/atom ratios as described for Ta₂O₅, up to the maximum ion/atom ratio tested of 0.69 at 300 eV.⁵⁷ Tested as an Al₂O₃/SiO₂ antireflective coating, 300 eV ion assist resulted in some reduced moisture absorption and increased abrasion resistance (but less abrasion resistance than Al₂O₃/SiO₂ and Ta₂O₅/SiO₂ antireflective coatings tested at the same time).

5. ENERGY-SPECIFIC APPLICATIONS (~50-1000 eV)

5.1 Self-limiting oxide layers

The oxidation of reactive metals such as Nb is used to form thin insulating layers for superconducting tunnel junctions⁴ and other surface-modification applications. Since the tunneling current decreases exponentially with increasing oxide thickness, it is desirable to provide a self-limiting oxide growth process, which is achieved using ion bombardment during oxidation. A simple model for oxide thickness uses an exponentially decreasing growth rate with increasing thickness plus a constant sputter removal rate imposed by the ion bombardment.⁴ The rate of change of thickness with time is given by

$$dx/dt = K \exp(-x/x_o) - S, \quad (1)$$

where x is the oxide thickness, S is the sputter removal rate, K is the initial oxidation rate, and X_o is a characteristic diffusion distance that depends on the oxide growth mechanism and temperature. Note that the ion beam may be entirely O₂⁺ or a mixture of O₂⁺ and Ar⁺, for example, to vary the balance between growth and removal. Under the conditions reported,⁴ it was found that varying the O₂⁺ ion energy from 45 to 180 eV gave self-limiting oxide layers that varied in junction resistance from about 10 to 10⁵ Ω. It was found that an ion energy of 180 eV gave no significant oxide growth, i.e., an upper limit to the ion energy for self-limiting oxide growth. To obtain the self-limiting oxide thicknesses, we would need specific values of x_o and K , which are not available. However, using parameters derived from other Nb oxidation studies, these values indicate self-limiting oxide thicknesses in the tens of Å range. Similar behavior has been reported in the nitridation of Si using 500 eV N₂⁺ ions which gave a self-limiting thickness of 19 Å.⁶¹

5.2 Film microstructure orientation

An ion energy sufficient to select a preferred microstructure orientation is sufficient to cause some lattice damage. At the same time, an energy that is too great will not be selective enough. There appears to be an intermediate energy that is optimum for selecting microstructure orientation. Several mechanisms that generate in-plane orientation in body-centered-cubic metal thin films have been described.⁶² It is also clear from examples with metal oxides that in-plane alignment can start in the early coalescence stage (e.g., MgO⁶³) or may require extended competition of grain orientations to become well developed (e.g., yttria-stabilized ZrO₂⁶⁴).

5.2.1 Aluminum - neon ions. This is a theoretical study that is included to help understand the grain alignment mechanisms.⁶⁵ The Al atoms were deposited with an energy of about 1 eV. The Ne⁺ ions had an energy of about 450 eV and an ion/atom arrival rate of 0.5. The two mechanisms compared were (1) preferential sputtering of differently oriented grains and (2) preferential damage of differently oriented grains followed by grain-boundary migration. Both mechanisms were found capable of producing alignment. But the second mechanism resulted in much more rapid alignment and is believed to be the dominant mechanism, except where grain boundaries have very low mobility, as in many ceramics.

5.2.2 Cobalt-platinum. Vapor deposited Co and Pt were used to grow CoPt₃ films nominally 600 Å thick at rates of 0.05-0.5 Å/s, with ion assist provided by 50 or 100 eV Ar⁺ ions with ion/atom ratios between 0 and 4.⁶⁶ Without ion assist, CoPt₃ films are known to exhibit room-temperature perpendicular magnetic anisotropy when deposited at 200-400°C. With ion assist and a 100°C substrate temperature, there was a small room-temperature enhancement at 100 eV, but a substantial one at 50 eV with an ion/atom ratio of 0.8. Other tests at ion energies greater than 100 eV indicate that 50 eV is the optimum of the energies investigated. At 250 and 400°C, there is reduced anisotropy at all ion energies investigated.

5.2.3 Copper. Films of Cu, 5-6 μm thick, were vapor deposited at rates of 6-20 Å/sec, using 62, 125, and 600 eV Ar⁺ ion assist over a range of ion/atom ratios.³² Alignment, shown by the (111)/(200) peak-intensity ratio, was superior at 125 eV, and reached near-saturation values at doses of only 2-3 eV/atom. With a SiO₂ substrate, the ratio exceeded 10² and with a

Si(100) substrate it exceeded 10^3 , with both substrates at 82°C . It was possible to reach an alignment ratio of 10^2 at 62 eV with a Si(100) substrate, but a dose of about 25 eV/ion was required. It was also possible to reach alignment ratios >10 for 600 eV, but the peak alignment was obtained at doses of several eV/atom and dropped considerably at higher doses.

5.2.4 Niobium. Films of Nb were sputter deposited to thicknesses of several hundred μm at a rate of $1.25 \text{ \AA}/\text{sec}$ on fused silica substrates using ion assist by 200 eV Ar^+ ions that were directed 20 degrees from a glancing angle with the deposition surface.^{67,68} The alignment corresponded to a channeling direction for incident ions between (110) planes. The degree of alignment increased slowly up to an ion/atom ratio of 0.5, and more rapidly thereafter. At an ion/atom arrival rate of 1.3, about half of the film grains were aligned within 5 degrees of the ion-beam direction. The sputter yield of the Nb during this deposition was about 0.6 atoms per incident ion. Major features of the alignment process were qualitatively predicted by theoretical calculation based on the dependence of sputter yield on grain orientation.⁶⁹

5.2.5 Magnesium oxide. Films of MgO were vapor deposited on amorphous Si_3N_4 substrates with ion assist by 700 eV Ar^+ ions.⁶⁵ The angle between the ion beam and the substrate was 45 degrees, which is a channel direction for (100) MgO. In-plane textured films have been obtained at room temperature to 300°C . For room temperature, the best alignment was obtained with a $1.5 \text{ \AA}/\text{s}$ evaporation rate. Based on this rate, the ion/atom ratio was 0.43-0.47 and the energy dose was 300-330 eV/atom. The in-plane alignment had an angular width as small as 7 degrees in films as thin as 100 \AA . It appeared that the deposition started with aligned crystallites, as opposed to a non-aligned film. These thin, aligned films have potential as structural templates in manufacturing processes.

In another study, films of MgO were vapor deposited at a rate of $1.7 \text{ \AA}/\text{s}$ on 30 nm thick Si_3N_4 substrates at room temperature, with ion assist by 750 eV Ar^+ ions.⁷⁰ The angle between the ion beam and the substrate was again 45 degrees. With an ion/atom ratio of 0.22 and an energy dose of 160 eV/atom, the formation of aligned crystallites, as indicated by RHEED images, began at a film thickness of 37 \AA and was completed at a thickness of 48 \AA . In other experiments,⁷⁰ alignment was observed for ion energies from 500-1100 eV and ion-atom ratios of 0.11-0.29.

5.2.6 Titanium nitride - vapor deposited Ti. Films of Ti were vapor deposited at $3.3 \text{ \AA}/\text{sec}$ on Si(111) substrates to grow TiN, 700 nm thick, using ion assist by 2 keV N^+ and N_2^+ ions at $50 \mu\text{A}/\text{cm}^2$ with and without UV light (wavelength between 235 and 450 nm) at an intensity of $360 \text{ mW}/\text{cm}^2$ in an N_2 background pressure of 0.015 Pa.⁷¹ Calculating a TiN deposition rate of $3.7 \text{ \AA}/\text{s}$ from the Ti deposition rate, at normal incidence the ion/atom ratio was 0.084 with an energy dose of 167 eV/atom, and the UV energy dose was 600 eV/atom. Using ion assist only at normal incidence, a {111} orientation of the crystallites was obtained. An ion incidence 55 degrees from normal reduced the ion/atom ratio to 0.048 and the ion energy dose to about 100 eV/atom and produced both a {111} orientation relative to the surface and a {100} orientation relative to the ion beam, which totally fixed the crystallite orientation. The simultaneous use of UV radiation in the 55 degree configuration promoted a uniformly oriented growth. This work included an ion energy greater than the 1 keV limit for the rest of this paper, but is an interesting addition to the other crystallite alignment work presented.

5.3 Selection of preferred crystal structure

Growth of cubic boron nitride (c-BN) in thin films by the vapor deposition of B and the bombardment by 300, 500, and 800 eV N_2^+ (and some N^+) ions requires the simultaneous meeting of conditions.^{72,73} There is the obvious requirement that a stoichiometric number of N_2^+ and N^+ ions arrive to combine with the B. There is a minimum temperature of $200\text{-}300^\circ\text{C}$ for the formation of c-BN films. There is also an optimum temperature range of $400\text{-}500^\circ\text{C}$. Epitaxial growth did not occur. Instead, transitional films of amorphous and hexagonal BN were required before c-BN would grow. Growth was demonstrated on Ni, Si, and diamond substrates. The growth of c-BN also involved the development of substantial compressive stress, possibly due to Ar interstitials. Films of c-BN could not be grown on Cu(100) substrates, even though the lattice mismatch with c-BN was small, probably due to its high ductility.

The growth of c-BN also required a threshold momentum per deposited boron atom of 200, measured in units of $(\text{eV}\times\text{amu})^{1/2}$. As an example, for a typical ion energy of 500 eV, this required an N_2^+ to boron atom arrival rate of 1.7. This would be 850 eV per boron atom or, the way energy dose is calculated in the rest of this paper, 425 eV/atom. There is

also a sputtering threshold, typically only 50 percent higher than the threshold for deposition of c-BN, where the sputtering by the ion beam prevents any deposition.

A persuasive demonstration that momentum was involved, rather than energy, was made by using mixtures of nitrogen ions and Ar⁺, Kr⁺, and Xe⁺ ions. The combined momentum per boron atom was obtained by summing the product (eV×amu)^{1/2}(ion/atom) for all the ions. While the argument for the importance of momentum in the production of c-BN was persuasive, there is no basis for assuming a similar importance of a momentum parameter in substantially different processes. For example, the crystal structures of metal films could be sharply different under 50 and 300 eV Ar⁺ ion bombardment, even if the momentums of the two doses were adjusted to be the same.

5.4 Ohmic contacts on semiconductors

Cleaning Gallium arsenide with 50, 300, and 500 eV Ar⁺ ions was followed by forming diodes on the cleaned surface.²⁶ The diodes on the surfaces cleaned at 50 and 300 eV showed minor and substantial degradation of diode performance. The diodes on the surfaces cleaned at 500 eV showed ohmic contacts with no diode characteristics. The transition to ohmic contact for GaAs thus occurred between 300 and 500 eV, indicating that the polycrystalline surface produced by energetic ion bombardment can provide ohmic contact to a semiconductor. Higher energies should be undesirable in that unnecessary damage would be done to the semiconductor.

6. CONVERSION RELATIONSHIPS

The ion/atom ratio has been used throughout this paper. This parameter is preferred over the ratio of the experimental parameters of ion current density and deposition rate for the comparison of different ion-assist processes. The practical utilization of the processes described in this paper, however, requires conversion between the parameters used in this paper and the experimental parameters. For the reader's convenience, the ion-arrival rate in ions/cm²-s is

$$R_i = i_i/1.602 \times 10^{-19}, \quad (2)$$

where i_i is the ion current density in A/cm², and 1.602×10^{-19} is the electronic charge in C. Equation (2) assumes singly charged ions, which is true for most ion sources and most working gases (N₂⁺ and O₂⁺ for N₂ and O₂). The atom arrival rate in atoms/cm²-s is

$$R_a = 10^{-8} R_A \times \rho N / (1.66 \times 10^{-24} \times w), \quad (3)$$

where R_A is the film growth rate in Å/s, ρ is the density in g/cm³, N is the number of atoms in the molecule being deposited (1 for an element), w is the atomic weight of the molecule being deposited, and 1.66×10^{-24} is the mass in g of one amu. The ion/atom ratio is R_i/R_a . The energy dose in eV/atom is the ion/atom ratio times the ion energy in eV. If the thickness of an atomic layer in Å is needed, it is,

$$t_a = 10^8 [\rho N / (1.66 \times 10^{-24} \times w)]^{-1/3}. \quad (4)$$

As an example, SiO₂ has a density, ρ , of 2.26 g/cm³, a molecular weight, w , of 60.08, and the number of atoms per molecule N is 3. For a SiO₂ deposition rate R_A of 3 Å/s, $R_a = 2.04 \times 10^{15}$ atoms/cm²-s and $t_a = 2.45$ Å. For an ion current density i_i of 30 μA/cm², $R_i = 1.88 \times 10^{14}$ atom/cm²-s. The ion/atom ratio is $R_i/R_a = 0.092$. For a 100 eV ion energy, the energy dose would be 9.2 eV/atom. The ion current distribution and energy should be available from the manufacturer of the ion source, or it can be measured with probes. Experimental values of density, ρ , will vary from the theoretical value, but the error will probably be less than other errors in the calculations.

7. CONCLUDING REMARKS

The organization of ion-assist applications by energy is useful. The very-low-energy regime (~0-25 eV) is where bulk lattice atoms are not disturbed and the process is confined primarily to the surface. The low-energy regime (~25-100 eV)

is where bulk lattice atoms are affected by large-amplitude lattice vibrations (described by the molecular-dynamics theoretical approach), but lattice damage and gas implantation from ion assist is small. The high-energy regime (~100-1000 eV) involves much more damage and gas implantation and is a transitional regime extending from the lower limit where large-amplitude lattice vibrations are the dominant assist mechanism to the upper limit where the two-body collision-cascade approach is a more dominant assist mechanism. The bulk of ion-assist applications, not including those that require either very low energies or specific energies, are best done in the low-energy regime. Many applications that are carried out at present in the high-energy regime are using high ion energies for historical ion-source availability reasons, not because the processes are performed better at high energy than at ≤ 100 eV.

REFERENCES

1. J.M.E. Harper, J.J. Cuomo, and H.R. Kaufman, *J. Vac. Sci. Technol.*, **21**, 737-756, 1982.
2. H. R. Kaufman, *J. Vac. Sci. Technol.*, **15**, 272-276, 1978.
3. H.R. Kaufman, J.J. Cuomo, and J.M.E. Harper, *J. Vac. Sci. Technol.*, **21**, 725-736, 1982.
4. A.W. Kleinsasser, J.M.E. Harper, J.J. Cuomo, and M. Heiblum, *Thin Solid Films*, **95**, 333-342, 1982.
5. T.M. Mayer, J.M.E. Harper, and J.J. Cuomo, *J. Vac. Sci. Technol.*, **A3**, 1779-1783, 1985.
6. J.E. Yehoda, B. Yang, K. Vedam, and R. Messier, *J. Vac. Sci. Technol.*, **A6**, 1631-1635, 1986.
7. H.R. Kaufman, R.S. Robinson, and R.I. Seddon, *J. Vac. Sci. Technol.*, **A5**, 2081-2084, 1987.
8. H. R. Kaufman and R. S. Robinson, "End-Hall Ion Source," *U.S. Patent* 4,862,032, 1989.
9. J.J. Cuomo, S.M. Rossnagel, and H.R. Kaufman, eds., *Handbook of Ion Beam Processing Technology*, Noyes Publications, Park Ridge, New Jersey, 1989.
10. F.A. Smidt, *International Materials Reviews*, **35**, 61-128, 1990.
11. J.M.E. Harper, J.J. Cuomo, R.J. Gambino, and H.R. Kaufman, pp. 127-162 in *Ion Bombardment Modification of Surfaces: Fundamentals and Applications* (O. Auciello and R. Kelly, eds.), Elsevier Science Publishers B.V., Amsterdam, 1984.
12. P.J. Martin and R.P. Netterfield, pp. 114-182 in *Prog. in Optics* (E. Wolf, ed.), Vol. 23, Elsevier Science Pub., Amsterdam, 1986.
13. I. Petrov, P.B. Barna, I. Hultman, and J.E. Greene, *J. Vac. Sci. Technol.*, **A21**, S117-S128, 2003.
14. G.K. Wehner and G.S. Anderson, pp. (3-1)-(3-38) in *Handbook of Thin Film Technology* (L.I. Maisel and R. Glang, eds.), McGraw-Hill Book Co., New York, 1970.
15. K. Ino, T. Shinohara, T. Ushiki, and T. Ohmi, *J. Vac. Sci. Technol.*, **A15**, 2627-2635, 1997.
16. J.-S. Chun, I. Petrov, and J.E. Greene, *J. Appl. Phys.*, **86**, 3633-3641, 1999.
17. V.V. Zhurin, H.R. Kaufman, J.R. Kahn, and T.L. Hylton, *J. Vac. Sci. Technol.*, **A18**, 37-41, 2000.
18. R.A. Roy and D.S. Yee, pp. 194-218 in Ref. 8.
19. K.-H. Muller, pp. 241-278 in Ref. 8.
20. E. Kay and S.M. Rossnagel, pp. 170-193 in Ref. 8.
21. H.R. Kaufman and J.M.E. Harper, *J. Vac. Sci. Technol.*, **A22**, 221-224, 2004.
22. L. Hanley and S. B. Sinnott, *Surf. Sci.*, **500**, 500-522, 2002.
23. 12-cm ion source with dished molybdenum grids, Commonwealth Scientific Corporation (presently marketed by Veeco Instrument Inc.).
24. EH1000 end-Hall ion source, Kaufman & Robinson, Inc.
25. C.D. Child, *Phys. Rev.*, **2**, 492-511, 1911.
26. J.R. Sites, Unpublished research report SF-26, 1979.
27. X.W. Zhou and H.N.G. Wadley, *J. Appl. Phys.*, **87**, 8487-8496, 2000.
28. X.W. Zhou and H.N.G. Wadley, *J. Appl. Phys.*, **87**, 2273-2281, 2000.
29. X.W. Zhou and H.N.G. Wadley, *J. Appl. Phys.*, **88**, 5737-5743, 2000.
30. R. Kelly, pp. 91-119 in *Handbook of Plasma Processing Technology* (S.M. Rossnagel, J.J. Cuomo, and W.D. Westwood, eds.), Noyes Publications, Park Ridge, New Jersey, 1990.
31. J.J. Cuomo, J.M.E. Harper, C.R. Guarnieri, D.S. Yee, L.J. Attanasio, J. Angilello, and C.T. Wu, *J. Vac. Sci. Technol.*, **20**, 349-354, 1982.
32. R.A. Roy, J.J. Cuomo, and D.S. Yee, *J. Vac. Sci. Technol.*, **A6**, 1621-1626, 1988.

33. J.E. Greene and S.A. Barnett, *J. Vac. Sci. Technol.*, **21**, 285-302, 1982.
34. D.S. Campbell, p. (12-1)-(12-50) in *Handbook of Thin Film Technology* (L.I. Maissel and R. Glang, eds.), McGraw-Hill Book Co., New York, 1970.
35. J.R. MacNeil, L.J. Wei, G.A. Al-Jumaily, S. Shakir, and J.K. McIver, *Applied Optics*, **24**, 480-485, 1985.
36. G.A. Al-Jumaily, "Influence of Metal Films on the Optical Scatter and Related Microstructure of Coated Surfaces," *Ph.D. Thesis*, Univ. of New Mexico, 1986. This publication includes information not in the preceding reference.
37. S. Masaki, M. Iwase, and H. Morisaki, *Nuclear Instr. Methods Phys. Res.*, **B37/38**, 846-849, 1989.
38. E.H. Hirsch and I.K. Varga, *Thin Solid Films*, **69**, 99-105, 1980.
39. M.L. Fulton, *SPIE*, **2253**, 374-393, 1994.
40. J.R. McNeil, personal communication.
41. A.S. Kao, C. Huang, V.J. Novotny, V.R. Deline, and G.L. Gorman, *J. Vac. Sci. Technol.*, **A7**, 2966-2974, 1989.
42. D.S. Yee, J. Floro, D.J. Mikalsen, J.J. Cuomo, K.Y. Ahn, and D.A. Smith, *J. Vac. Sci. Technol.*, **A3**, 2121-2128, 1985.
43. J.A. Thornton, *Ann. Rev. Mater. Sci.*, **7**, 239-260, 1977.
44. J.M.E. Harper, J.J. Cuomo, and H.T.G. Hentzell, *Appl. Phys. Lett.*, **46**, 547-549, 1983.
45. J.M.E. Harper, J.J. Cuomo, and H.T.G. Hentzell, *J. Appl. Phys.*, **58**, 550-555, 1985.
46. H.T.G. Hentzell, J.M.E. Harper, and J.J. Cuomo, *J. Appl. Phys.*, **58**, 556-563, 1985.
47. I.-H. Kim and S.-H. Kim, *J. Vac. Sci. Technol.*, **A13**, 2814-2818, 1995.
48. J.-S. Cho and S.-K. Koh, *J. Vac. Sci. Technol.*, **B21**, 2060-2066, 2003.
49. A.R. Buchel, M.G. Wohlwend, and M.L. Fulton, *Soc. Vac. Coaters, 36th Annual Tech. Conf. Proc.*, 82-87, 1993.
50. P.J. Martin, A. Bendavid, M. Swain, R.P. Netterfield, T.J. Kinder, W.G. Sainty, D. Drage, and L. Wielunski, *Thin Solid Films*, **239**, 181-185, 1995.
51. J.S. Colligan, *J. Vac. Sci. Technol.*, **A13**, 1649-1657, 1995.
52. R. Messier, A.P. Giri, and R.A. Roy, *J. Vac. Sci. Technol.*, **A2**, 500-503, 1984.
53. J.M.E. Harper, private communication.
54. H. R. Kaufman and R. S. Robinson, *Operation of Broad-Beam Sources*, Commonwealth Scientific Corporation, Alexandria, Virginia, 1987.
55. J.M.E. Harper, J.J. Cuomo, P.A. Leary, G.M. Summa, H.R. Kaufman, and F.J. Bresnock, *J. Electrochem. Soc.*, **128**, 1077-1083, 1981.
56. J.M.E. Harper and R.J. Gambino, *J. Vac. Sci. Technol.*, **16**, 1901-1905, 1979.
57. F.L. Williams, D.W. Reicher, C.-B. Juang, and J.R. McNeil, *J. Vac. Sci. Technol.*, **A7**, 2286-2288, 1989.
58. F.L. Williams, "Low Temperature Deposition of Thin Films Using Ion Assisted Deposition," *Ph.D. Thesis*, Univ. of New Mexico, 1989. This publication includes information not in the preceding reference.
59. M.S. Al-Robae, M.G. Krishna, K.N. Roa, and S. Mohan, *J. Vac. Sci. Technol.*, **A9**, 3048-3053, 1991.
60. M.S. Al-Robae, L. Shivalingappa, K.N. Roa, and S. Mohan, *Thin Solid Films*, **221**, 214-219, 1992.
61. J.A. Taylor, G.M. Lancaster, A. Ignatiev, and J.W. Rabalais, *J. Chem. Phys.*, **68**, 1776-1784, 1978.
62. J.M.E. Harper, K.P. Rodbell, and E.G. Colgan, *J. Appl. Phys.*, **82**, 4319-4326, 1997.
63. C.P. Wang, K.B. Do, M.R. Beasley, T.H. Geballe, and R.H. Hammond, *Appl. Phys. Lett.*, **71**, 2955-2957, 1997.
64. Y. Iijima, K. Onabe, N. Futaki, N. Sadakata, O. Kohno, and Y. Ikeno, *J. Appl. Phys.*, **74**, 1905-1911, 1993.
65. L. Dong and D.J. Srolovitz, *Appl. Phys. Lett.*, **75**, 584-586, 1999.
66. D. Vasumathi, B.B. Maranville, and F. Hellman, *Appl. Phys. Lett.*, **79**, 2782-2784, 2001.
67. L.S. Yu, J.M.E. Harper, J.J. Cuomo, and D.A. Smith, *Appl. Phys. Lett.*, **47**, 932-933, 1985.
68. L.S. Yu, J.M.E. Harper, J.J. Cuomo, and D.A. Smith, *J. Vac. Sci. Technol.*, **A4**, 443-447, 1986.
69. R.M. Bradley, J.M.E. Harper, and D.A. Smith, *J. Appl. Phys.*, **60**, 4160-4164, 1986.
70. R.T. Brewer and H.A. Atwater, *Appl. Phys. Lett.*, **80**, 3388-3390, 2002.
71. J.W. Gerlach, U. Prekwinkel, H. Wengenmair, T. Kraus, and B. Rauschenbach, *Appl. Phys. Lett.*, **68**, 2360-2362, 1996.
72. D.J. Kester and R. Messier, *J. Appl. Phys.*, **72**, 504-513, 1992.
73. D.J. Kester, K.S. Ailey, D.J. Lichtenwalner, and R.F. Davis, *J. Vac. Sci. Technol.*, **A12**, 3074-3081, 1994